ELSEVIER

Catalysis Today 34 (1997) 421–427

CATALYSIS TODAY

Chapter 12

Interaction between chemical kinetics and transport phenomena in monolithic catalysts

Enrico Tronconi

Politecnico di Milano, Department of Industrial Chemistry and Chemical Engineering, Piazza Leonardo da Vinci, 32 20133 Milano, Italy

1. Introduction

Analysis of the interactions between intrinsic kinetics of catalytic reactions and physical phenomena such as interphase and intraphase mass and heat transfer is one of the major topics of catalytic reactor engineering, being deeply involved in the development of many chemical processes.

This presentation is intended to illustrate theoretical approaches and experimental methods used in our laboratories to investigate such matters with respect to a specific process of great industrial relevance, namely the selective catalytic reduction (SCR) with ammonia of nitrogen oxides present in the flue gases of power stations. A peculiarity of this problem lies in the fact that the catalytic material is used in the shape of monoliths rather than in pellets as in more conventional catalytic processes of the Chemical Industry. This results in somewhat simplified geometrical and fluodynamic aspects, making the problem an appropriate example for teaching purposes.

In the following we first outline the most important characteristics of monolithic catalysts used in the $DeNO_x$ SCR process. Then we proceed to derive a one-dimensional mathematical description of transport phenomena in monolithic matrices, including gas–solid mass transfer as well as intraporous diffusion. On combining it with the rate equation representative of intrinsic $DeNO_x$ kinetics one obtains a comprehensive model of the monolithic SCR reactor, whose validation is then demonstrated via the following steps: (a) estimation of the parameters of the $DeNO_x$ rate equation from kinetic data obtained in a chemical regime; (b) determination of the effective intraporous diffusivities of NO and NH_3 in the monolith catalyst; (c) comparison of model predictions with data collected in a laboratory monolith reactor representing the influence of the operating variables on NO_x conversion. A final section is devoted to show how this mathematical treatment can be applied to analyze the influence of the catalyst pore structure, an aspect relevant to the rational design of SCR catalysts.

1.1. Properties of monolithic catalysts for $DeNO_x$ SCR process

1.1.1. Selective catalytic reduction of nitrogen oxides

Air pollution caused by the emission of nitrogen oxides in stack gases from stationary sources, mainly from thermal power stations, is at present the object of major concern, such emissions accounting for one third of man made NO_x and being blamed for the production of

PII S0920-5861(96)00064-8

acid rains and for other environmental problems. Among flue gas treatment methods for controlling NO_x emissions, selective catalytic reduction (SCR) is most widely used due to its efficiency, selectivity and economics. The SCR technology has been extensively reviewed in recent years (Bosch and Janssen, 1988; Forzatti and Bregani, 1991), and its general aspects are beyond the scope of this presentation. Briefly, it is based on the reduction of NO_x (mostly NO) with NH_3 into innocuous water and nitrogen according to the following main reaction:

$$4NO + 4NH_3 + O_2 \rightarrow 4N_2 + 6H_2O \quad (1)$$

Liquid ammonia is vaporized, diluted with air and injected into the flue gas stream through a distribution grid prior to the SCR reactor. Reaction (1) occurs over honeycomb or plate-type monolith catalysts consisting of homogeneous mixtures of titanium dioxide, tungsten oxide, vanadium pentoxide and silico-aluminates. TiO_2 anatase (80% w/w) is used to support the active material, with vanadia (< 2% w/w) being primarily responsible for the activity of the catalyst both in the reduction of NO_x and in the undesired oxidation of SO_2 to SO_3. WO_3 (10% w/w) provides the catalyst with higher thermal stability, whereas silico-aluminates and ceramic fibers are added to ensure the desired mechanical and ceramic properties.

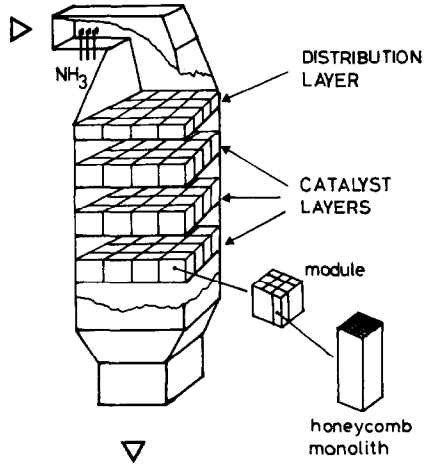

Fig. 1. Structure of SCR reactors.

Table 1
Comparison of external surface area of conventional packing and monolithic structures

Catalyst type	Geometric surface area (m^2/m^3)
Ceramic hollow cylinders,	
15×15×2 mm	330
Alumina pellets,	
5×5 mm	1200
Commercial SCR honeycomb,	
150×150×1000 mm:	
20×20 cells	427
40×40	862
Corrugated honeycomb, Engelhard:	
1/3 in. wavelength	1100
1/7 in.	2800
1/10 in.	4900

1.1.2. Characteristics of monolithic structures

Ceramic honeycomb monoliths are obtained by extruding a mass of paste-like catalytic material, while plate-type monoliths are made by depositing the catalytic material onto a stainless steel net or a perforated metal plate. Fig. 1 shows a typical SCR reactor with ceramic honeycomb catalysts assembled in modules. Each module contains a large number of parallel straight channels with openings of few millimetres. Similar monolithic structures are used also in the control of automotive emissions (catalytic mufflers) and in the abatement of waste exhaust gases (catalytic incinerators). The reasons for choosing catalysts with monolithic structures rather than the usual packed-bed concept have been rationalized already during the '70s (Hlavacek and Votruba, 1976), and can be summarized as follows.

(i) A major advantage of the honeycomb matrix is a very low pressure drop due to the existence of straight channels in the monolith matrix: in a packed bed with the same external geometric surface area the pressure drop may be greater by two to three orders of magnitude.

(ii) In packed beds where very fast catalytic reactions occur only the external geometric surface area of the catalyst particles is active, the reaction zone being confined to a narrow outer shell because of the strong intraporous diffu-

sional limitations; this is the reason why special geometries of the catalyst pellets ensuring short diffusion paths (e.g. hollow cylinders, or "rings") are adopted. In comparison with packed beds, monolithic supports may have higher geometric surface area, as shown in Table 1.

(iii) Most important in the treatment of flue gases, honeycomb supports are attrition-resistant, as well as resistant to deposition of carbon and dust.

1.2. Mathematical description of chemical kinetics and transport processes in monolithic SCR catalysts

1.2.1. Rate of the $DeNO_x$ reaction

Basic to the design of SCR monolithic catalysts is the knowledge of the rates of chemical changes involved in the $DeNO_x$ reaction, as well as their dependencies on concentrations and temperature. Such knowledge is summarized by a rate expression which can be incorporated into the global mathematical model of the monolith reactor. In line with mechanistic and kinetic evidence concerning the role of strongly adsorbed ammonia in the catalytic reduction of NO (Ramis et al., 1990), we have selected a Rideal-type rate equation (Tronconi et al., 1992):

$$r_{NO} = k_{NO} C_{NO} \frac{K_{NH_3} C_{NH_3}}{1 + K_{NH_3} C_{NH_3}} \qquad (2)$$

Eq. (2) implies that either weakly adsorbed or gaseous NO reacts with NH_3 strongly adsorbed on the catalyst surface. Kinetic dependencies on O_2 and H_2O are neglected on the basis of experimental evidence obtained under typical SCR conditions. Rate Eq. (2) contains two adaptive parameters (k_{NO} and K_{NH_3}), which must be estimated in the absence of diffusional disguises for Eq. (2) to be representative of intrinsic $DeNO_x$ kinetics. This aspect is further discussed in the following Section 3. Notably, rate Eq. (2) reduces to first order kinetics in NO for $K_{NH_3} C_{NH_3} \gg 1$, as observed in the case of NH_3 excess, but can represent also kinetic dependencies on NH_3 resulting from reaction mixtures with substoichiometric NH_3/NO ratios, as used in the industrial practice ($K_{NH_3} C_{NH_3} \ll 1$).

1.2.2. Transport mechanisms in SCR monolith structures

In monolithic SCR catalysts the reactants flow along the matrix channels, usually in a laminar regime, and the reaction products are carried away by the flow of the gas stream. The rate of the overall process involves two steps in series: (i) the transport process of the reactants NO and NH_3 between the bulk flow and the surface of the catalytic walls of the channel (external field); (ii) the simultaneous diffusion and reaction of NO and NH_3 inside the porous walls of the matrix (internal field). Thermal effects are virtually negligible due to the very small concentrations of the reactants NO and NH_3, so that isothermal operation of the catalyst can be assumed. If it is further supposed that conditions are perfectly uniform in all the channels of the monolith structure, then the one-dimensional governing equations of a SCR monolithic catalyst can be readily derived from steady-state mass balances of NO and NH_3 for the external and the internal field in a single monolith channel.

1.2.3. Equations for the external field

· Gas-phase mass balance of NO:

$$u_{av} \frac{dC_{NO,b}}{dz} = -\frac{4}{d_h} k_{mt,NO} (C_{NO,b} - C^*_{NO}) \qquad (3)$$

with initial condition: $C_{NO,b} = C^0_{NO,b}$ at $z = 0$.

· Gas-phase mass balance of NH_3:

$$C^0_{NO,b} - C_{NO,b} = C^0_{NH_3,b} - C_{NH_3,b} \qquad (4)$$

In Eq. (3) z is the axial coordinate, $C_{j,b}$ and C^*_j are concentrations of species j in the bulk of the gas phase and on the surface of the catalytic wall, respectively, u_{av} is the average flow velocity, d_h the hydraulic diameter of the monolith channel, k_{mt} a mass transfer coefficient. Eq.

(3) states that at any axial location z in the monolith channel the rate of change of the convective flux of NO in the gas phase equals the rate of NO diffusion to the catalytic wall. Axial dispersion of NO is neglected because it is of minor importance as compared to convective transport under typical conditions. According to Eq. (4), the consumption of NH_3 equals everywhere the consumption of NO due to the stoichiometry of Reaction (1).

1.2.4. Evaluation of interphase mass transfer rates

Notably, Eqs. (3) and (4) reflect a "lumped" approach, where average values of the bulk gas-phase concentration of NO and NH_3 over each cross section along the monolith channel, $C_{NO,b}$ and $C_{NH_3,b}$, are considered. Thus, all of the complexities associated with the description of the actual concentration gradients in the gas-phase resulting from gas–solid diffusion are lumped into a phenomenological interphase mass transfer coefficient, $k_{mt,NO}$. By virtue of the laminar flow regime prevailing in the monolith channels and of the well-defined geometry of the monolith matrix, however, this problem lends itself to a theoretical analysis. We have investigated the dependence of k_{mt} on fluodynamic and geometric variables and on the kinetics of the $DeNO_x$ reaction by solving numerically the equations of the external field in their rigorous multi-dimensional formulation (Tronconi and Forzatti, 1992). Essentially, the results confirm the validity of resorting to the analogy between heat and mass transfer, so that prediction of k_{mt} can be effected successfully on the basis of the well-known Graetz–Nusselt problem dealing with heat transfer to a fluid in laminar flow in ducts with constant wall temperature (Shah and London, 1978). The resulting formula is

$$k_{mt}d_h/D = Nu_{\infty,T} + 8.827(1000z^*)^{-0.545}\exp(-48.2z^*) \quad (5)$$

where $z^* = (zD/u_{av}d_h^2)$ is a dimensionless axial coordinate and $Nu_{\infty,T} = 3.657$ for circular channels, $= 2.976$ for square channels and $= 2.47$ for equilateral triangles. By using Eq. (5) one can reproduce successfully experimental effects of the flow velocity and of the size of the monolith channels, which are strictly related to the role of gas–solid diffusional resistances, as shown for example in Fig. 2 and Fig. 3.

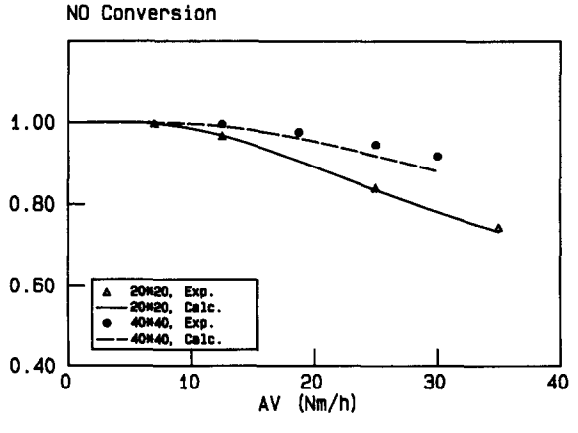

Fig. 2. Effect of "area velocity" AV = volumetric flow rate per unit geometric area on NO conversion. Reproduced from Tronconi and Forzatti, 1992, with kind permission of the American Institute of Chemical Engineers.

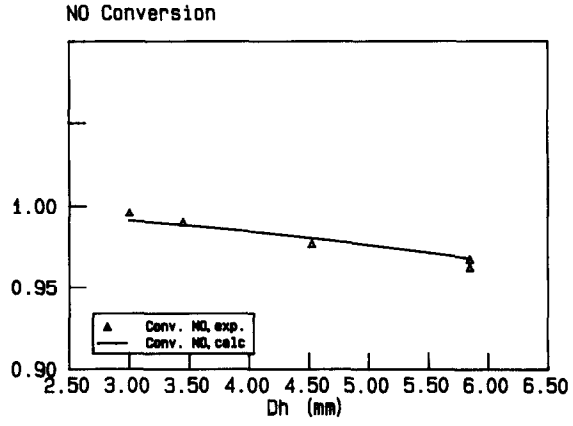

Fig. 3. Effect of channel hydraulic diameter d_h on NO conversion. Reproduced from Tronconi and Forzatti, 1992, with kind permission of the American Institute of Chemical Engineers.

1.2.5. Equations for the internal field

· Solid-phase mass balance of NO:

$$D_{e,NO} = \frac{d^2C_{NO}^*}{dx^2} = r_{NO}(C_{NO}^*, C_{NH_3}^*) \quad (6)$$

with boundary conditions:

$$x = 0: \frac{dC^*_{NO}}{dx} = 0;\ x = h:$$

$$D_{e,NO} = \frac{dC^*_{NO}}{dx} = k_{mt,NO}(C_{NO,b} - C^*_{NO})$$

· Solid-phase mass balance of NH_3:

$$D_{e,NH_3}\frac{d^2C^*_{NH_3}}{dx} = r_{NO}(C^*_{NO}, C^*_{NH_3}) \quad (7)$$

with boundary conditions:

$$x = 0: \frac{dC^*_{NH_3}}{dx} = 0;\ x = h:$$

$$D_{e,NH_3}\frac{dC^*_{NH_3}}{dx} = k_{mt,NH_3}(C_{NH_3,b} - C^*_{NH_3})$$

Eqs. (6)–(7) represent differential mass balances of the two reactants NO and NH_3 with effective intraporous diffusivities $D_{e,NO}$ and D_{e,NH_3} within a slice of catalyst wall with thickness dx perpendicular to the direction of flow. When combined with Eqs. (2)–(5) they provide a system of coupled differential and algebraic equations whose solution yields the axial profiles of $C_{NO,b}$ and $C_{NH_3,b}$ along the monolith matrix. At each integration step along the axial coordinate such computations require solution of a boundary-value problem, Eqs. (6)–(7), using orthogonal collocations (Finlayson, 1980). Solution of the global model equations for given geometric, kinetic and diffusional parameters provides predictions of such industrially relevant quantities as NO conversion and NH_3 outlet concentration ("NH_3 slip"). An approximate analytical solution of Eqs. (6)–(7) is presented by Tronconi et al. (1992).

1.2.6. Estimation of effective intraporous diffusivities

$D_{e,NO}$ and D_{e,NH_3} can be determined experimentally or estimated from a suitable model of diffusion inside the pore structure of the monolith catalyst. In fact Beekman (1991) has reported a satisfactory agreement between experimental diffusion coefficients in commercial SCR monoliths and values calculated according to the so called "random pore model" proposed by Wakao and Smith (1962). We have implemented the same approach, which allows to handle diffusion in porous structures with bimodal pore size distribution, as exhibited by the most recent SCR catalysts.

1.3. Estimation of $DeNO_x$ intrinsic kinetic parameters

Intrinsic kinetic data for the $DeNO_x$ reaction have been collected over a commercial SCR catalyst after grinding the honeycomb matrix to very fine particles in order to avoid internal diffusional limitations (Tronconi et al., 1992). The data were obtained in a conventional integral isothermal flow microreactor loaded with 1.9 g of catalyst and operated at $P = 1.6$ bar, $T = 200$–300°C, feed flow rate = 300 l/h and a feed composition simulating actual power plant SCR conditions (500 ppm NO, 600 ppm NH_3, 500 ppm SO_2, 2% v/v O_2, 10% v/v H_2O + balance N_2). Since $\alpha = NH_3/NO > 1$, the data could be analyzed assuming first order in NO and zero order in NH_3. Fig. 4 shows Arrhenius plots of the rate constant k_{NO} for two different particle sizes: the two plots diverge in the high-T region suggesting that data obtained over the

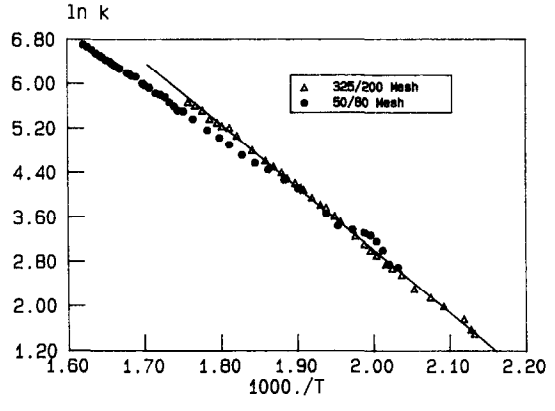

Fig. 4. Arrhenius plots of $DeNO_x$ kinetic data obtained over a commercial SCR catalyst ground to particles. Reprinted from Tronconi et al., 1992, with kind permission from Elsevier Science B.V.

50/80 mesh particles could be still affected by intraparticle diffusional intrusions. Analysis of the data for the 200/325 mesh particles provides

$$k_{NO} = 1.28 \times 10^{+11} \exp(-22400/(RT))\ s^{-1} \quad (8)$$

Notice that the estimated activation energy exhibits the expected order of magnitude for intrinsic chemical kinetics and agrees with other published results. The estimate of K_{NH_3} is much less critical and was determined by fitting directly the data obtained over the monolithic catalyst.

1.4. Validation of the mathematical model

Model predictions of NO conversion in a monolith reactor based on the above parameter estimates are compared in Fig. 5 with experimental measurements obtained over the same catalyst of the kinetic study, now shaped in the form of monoliths of various lengths, using a feed stream with 500 ppm NO, 500 ppm SO_2, 2% v/v O_2, 10% $H_2O + N_2$ (Svachula et al., 1993). Fig. 6 further demonstrates the model adequacy in relation to the effect of the NH_3/NO feed ratio at two distinct temperatures.

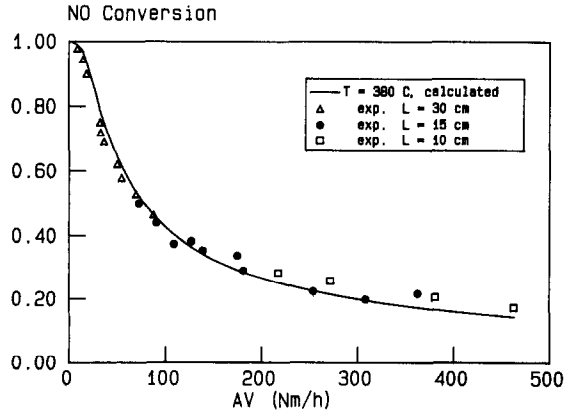

Fig. 5. Effect of monolith length and of AV; $d_h = 6$ mm, $\alpha = 1.2$, $T = 380$°C. Reprinted from Tronconi et al., 1992, with kind permission from Elsevier Science B.V.

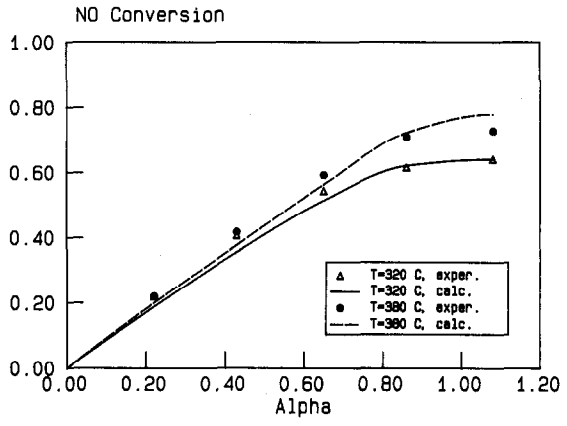

Fig. 6. Effects of and T; $d_h = 6$ mm, $AV = 33$ Nm/h. Reprinted from Tronconi et al., 1992, with kind permission from Elsevier Science B.V.

1.5. Influence of catalyst pore structure

The strong intraporous diffusional limitations prevailing in SCR catalysts suggest the opportunity to improve the NO_x removal efficiency by optimization of the catalyst morphology. For a bimodal (micro + macro) pore size distribution Fig. 7 shows the calculated influence of changing the fraction of micropores, ϵ_{mi}, for a fixed total catalyst void fraction = 0.7 ensuring the desired mechanical properties. A maximum is apparent at $\epsilon_{mi} \cong 0.4$ resulting from a balance between enhancing intraporous diffusivities of NO and NH_3 and increasing the catalyst specific surface area, as illustrated in Fig. 8. Such

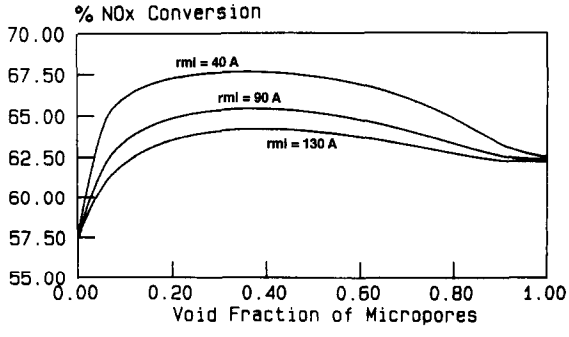

Fig. 7. Calculated NO conversion vs. micropore void fraction for different values of micropore radius r_{mi}; macropore radius = 2000 Å.

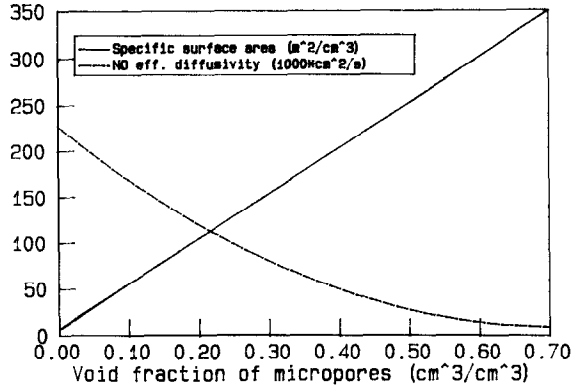

Fig. 8. Influence of ϵ_{mi} on catalyst specific surface area and on effective intraporous diffusivity of NO.

results provide practical guidelines for improving the design of SCR catalysts. It is estimated that up to 17% of the catalyst volume can be saved in comparison with a catalyst with monomodal pore size distribution and $r_{mi} = 130$ Å (Beretta et al., 1994).

2. Conclusions

We have shown how the interaction between chemical kinetics and transport processes in catalytic monolith SCR reactors can be successfully described starting from first principles and avoiding unnecessary empiricism due to the simple and well-defined system geometry in comparison, e.g. with packed beds. The model development has proceeded through the usual steps of model derivation, solution of the model equations, validation against suitable experimental data and application to design and optimization purposes. Under this respect the approach is standard and can be extended to similar problems involving different reactions, different catalyst characteristics and different reactor configurations.

In addition to the methodological approach, the example discussed in the previous Sections demonstrates a number of fundamental topics in chemical reactor engineering, including e.g. estimation of rate parameters through dedicated kinetic runs with negligible diffusional intrusions, the analogy between heat and mass transfer for evaluation of interphase mass transfer rates, and the evaluation of intraporous diffusivities by a suitable model of the pore structure.

Finally, it is worth stressing that development of a model for a reacting system may be a fruitful exercise. The model can be applied at least tentatively to identify optimal configurations for geometric and morphological properties of the catalyst. While a sound working experience does certainly provide the most efficient guidance in this respect, it can oftentimes be effectively supported and complemented by a careful implementation of a quantitative modelling approach.

Acknowledgements

The development of the SCR reactor model was performed under contract with ENEL/DSR/CRT (Pisa).

References

Beekman, J.W., I&EC Res., 30 (1991) 430.
Beretta, A., E. Tronconi, L.J. Alemany, J. Svachula and P. Forzatti, in V. Cortés Corberan and S. Vic Bellòn (Eds.), New Developments in Selective Oxidation II, Elsevier, 1994, p. 869.
Bosch, H., and F. Janssen, Catal. Today 2 (1988) 369.
Forzatti, P., and F. Bregani, La Termotecnica, Nov. 1991, p.57.
Hlavacek, V., and J.J. Votruba, in L. Lapidus and N.R. Amundson (Eds.), Chemical Reactor Theory – A Review, Prentice-Hall, 1976, p. 314.
Ramis, G., G. Busca, F. Bregani and P. Forzatti, Appl. Catal., 64 (1990) 259.
Shah, R.K., and A.L. London, Laminar Flow Forced Convection in Ducts, Academic Press, New York, 1978.
Svachula, J., N. Ferlazzo, P. Forzatti, E. Tronconi and F. Bregani, I&EC Res., 32 (1993) 1053.
Tronconi, E., and P. Forzatti, AIChE J., 38 (1992) 201.
Tronconi, E., P. Forzatti, J.P. Gomez Martin and S. Malloggi, Chem. Eng. Sci., 47 (1992) 2401.
Wakao, N., and J.M. Smith, Chem. Eng. Sci., 17 (1962) 825.